Front. Environ. Sci. Eng. 2020, 14(3): 40
https://doi.org/10.1007/s11783-020-1215-3

RESEARCH ARTICLE

Performance and mechanistic study on electrocoagulation process for municipal wastewater treatment based on horizontal bipolar electrodes

Zhenlian Qi[1], Shijie You (✉)[1], Ranbin Liu[2], C. Joon Chuah[3]

1 State Key Laboratory of Urban Water Resource and Environment, Harbin Institute of Technology, Harbin 150090, China
2 Sino-Dutch R&D Centre for Future Wastewater Treatment Technologies/Beijing Advanced Innovation Center of Future Urban Design, Beijing University of Civil Engineering & Architecture, Beijing 100044, China
3 Nanyang Environment and Water Research Institute, Nanyang Technological University, 1 Cleantech Loop, CleanTech One, Singapore 637141, Singapore

HIGHLIGHTS

- EC modified with BPEs enhances pollutant removal and reduce energy consumption.
- Increasing BPE number cannot increase flocculants yield exponentially.
- Simulations help to predict the distribution of electrochemical reactions on BPEs.

GRAPHIC ABSTRACT

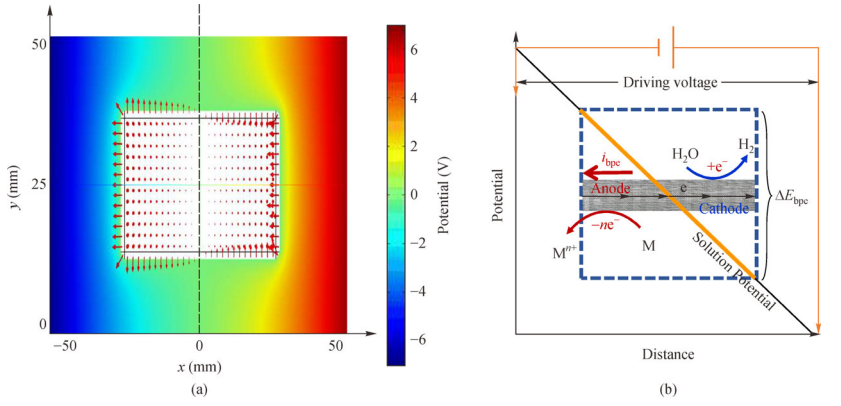

ARTICLE INFO

Article history:
Received 30 October 2019
Revised 17 December 2019
Accepted 5 January 2020
Available online 20 February 2020

Keywords:
Electrocoagulation
Bipolar electrodes
Municipal wastewater
Simulations

ABSTRACT

The design of electrodes is crucial to electrocoagulation process (EC), specifically, with respect to pollutant removal and energy consumption. During EC, the mechanisms for interaction between different electrode arrangement and electrode reactions remain unclear. This work presents an integrated EC process based on horizontal bipolar electrodes (BPEs). In the electrochemical cell, the graphite plates are used as driving cathode while either Fe or Al plates serves as driving anode and BPEs. The BPEs are placed horizontally between the driving electrodes. For municipal wastewater treatment, the pollutant removal efficiency and energy consumption in different configurations of two-dimension electrocoagulation (2D-EC) system with horizontal BPEs were investigated. The removal efficiency of turbidity, total phosphorus and total organic carbon increased significantly with the number of BPEs. Noted that the energy consumption for TP removal decreased by 75.2% with Fe driving anode and 81.5% with Al driving anode than those of 2D-EC, respectively. In addition, the physical field simulation suggested the distributions of potential and current in electrolyte and that of induced charge density on BPE surface. This work provides a visual theoretical guidance to predict the distribution of reactions on BPEs for enhanced pollutant removal and energy saving based on electrocoagulation process for municipal wastewater treatment.

1 Introduction

Electrocoagulation (EC) is an electrochemical process that has been widely applied to remove various pollutants such as heavy metals, organic substances, bacteria and particulates (Mollah et al., 2001; Garcia-Segura et al., 2017). EC

✉ Corresponding author
E-mail: sjyou@hit.edu.cn

can be used for treating several types of wastewater, ranging from municipal wastewater to highly contaminated industrial wastewater (Moussa et al., 2017) by virtue of simple equipment and easy automation. A typical EC system is made up of two-dimensional (2D) electrodes with one anode and one cathode in an electrolytic cell (Gao et al., 2010; Moussa et al., 2017). Such configuration may have several limitations like low space-time ratio, slow mass transfer rate, and low current efficiency (Daneshvar et al., 2004; Ghosh et al., 2008). This may hamper scale-up engineered application of EC process for practical wastewater treatment (Al-Shannag et al., 2013; Bani-Melhem et al., 2017). Thus, it will be desirable to improve the design of electrochemical cell and the adoption of electrodes with larger surface area to optimize pollutant removal and energy consumption (Mollah et al., 2004; Sahu et al., 2014; Jiménez et al., 2016).

Currently, the most commonly adopted configuration of electrodes for EC reactor can be divided into monopolar and bipolar electrodes (BPEs) as illustrated in Fig. S1 (Kobya et al., 2007). The BPEs are driven by electric field in solution, which allows to control the number of arbitrary matrix electrodes simultaneously (Figs. S1(b) and S1(c)). This will make it much easier to handle and maintain than monopolar electrode (Fig. S1(a)) (Chow et al., 2009; Zhang et al., 2016). The BPEs can be placed either vertically (in a direction being perpendicular to electric field) or horizontally (in a direction being parallel to electric field) in the EC cell. However, most of studies only adopted the vertically placed configuration while less attention has been paid to the performance of horizontal form BPEs arrangement (Jiang et al., 2002; Modirshahla et al., 2008).

The physical field modeling is a helpful tool to provide mechanistic insight into the reactor design for a wide range of applications (Bhatti et al., 2009, 2011; Hakizimana et al., 2017). Majority of prior works mainly focused on statistical modeling, which aimed to improve removal of various model pollutants through predicting and optimizing operational parameters (Chavalparit and Ongwandee, 2009; Olmez-Hanci et al., 2012). These models may face challenge for the case of complicated interactions among different variables such as electric potential, current distribution and mass transfer (Hakizimana et al., 2017). Effort has also been devoted to computational fluid dynamics (CFD) modeling, which has proven to be a useful tool to simulate and predict fluid flow and current density (Martinez-Delgadillo et al., 2012; Vázquez et al., 2012, 2014). Nevertheless, this method may not be suitable for investigating electrochemical field involved in EC process as the CFD modeling considers only electrochemical reactions as a whole (Hakizimana et al., 2017). Hence, it will be highly desirable to develop a simulation method that takes into account of electrochemical processes involving charge transport, electrode/solution interface reaction, potential and current (Hakizimana et al., 2017).

The aim of this study was to investigate the influence of horizontal BPEs on electrochemical performances for treating municipal wastewater by employing different combination of BPEs (Fe or Al). The yield of flocculant ions, pollutants removal and energy consumption were evaluated. We also performed visual simulation and analyzed the distribution of potential and current in the electrolyte and charge density on BPEs surface by using COMSOL Multiphysics software.

2 Materials and methods

2.1 Reactor setup and operation procedures

For each cycle of electrocoagulation experiment, all the electrodes were newly prepared and 1000 mL real municipal wastewater was filled into the cell. The municipal wastewater was collected from the inlet plant of the Wenchang Municipal Wastewater Treatment (Harbin, China), the specifications of which were given in supporting information. The municipal wastewater was stored at 4°C prior to use. The conductivity of wastewater was adjusted to 1.67 mS/cm by using sodium sulfate (Na_2SO_4, Sinopharm, China) according to our previous study (Qi et al., 2017). The driving electrodes were operated at current of 0.50 A and reaction time of 10 min. During the test, a large number of tiny bubbles were produced on both driving electrodes and BPEs, which played a role in stirring the solution. The voltage output was recorded every two minutes and the samples were taken at the 10th minute for analysis. The pH of wastewater was adjusted to desired values by using 0.50 M sulfuric acid (H_2SO_4, Bejing Shiji, China) or 0.50 M sodium hydroxide (NaOH, Benchmark, China). The electrocoagulation reactor was schematically illustrated in Fig. 1 and its working mechanism was described in Supporting Information.

2.2 Analytical methods

During the test, the wastewater was mixed evenly, and then dissolved in 2 M perchloric acid ($HClO_4$, Beijing Shiji, China) for determination of total iron and total aluminum. The concentration of Fe and Al, total organic carbon (TOC), total phosphorus (TP), total nitrogen (TN), turbidity, conductivity and pH of the wastewater samples were analyzed according to the methods described in Supporting Information. The current output was recorded in the sixtieth second after the running of electrolysis. The surface morphology of Fe and Al electrode, the characterization of precipitate were examined by using Scanning Electron Microscope (SEM) equipped with energy

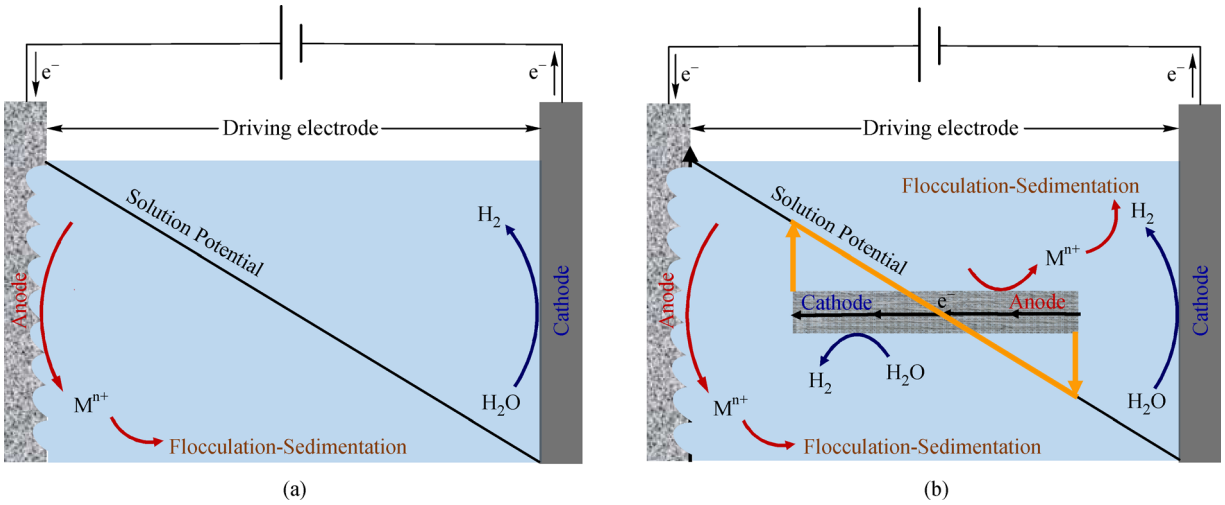

Fig. 1 Schematic illustration of (a) conventional two-dimension electrocoagulation and (b) the integration of electrocoagulation and horizontally placed BPE.

dispersive X-ray spectrometer (EDS) (Sirion 200, FEI, US). The electric energy consumption (EEC) of the electrocoagulation treatment was calculated according to Eq. (1) as

$$\mathrm{EEC}\left(\frac{\mathrm{kWh}}{\mathrm{kg}}\right)=\frac{1000UIt}{CV_{\mathrm{s}}}, \tag{1}$$

where t is the electrolysis time (h), I the output current (A), U the applied voltage (V), C the concentration of TOC, TP, or TN removed (mg/L) and V_{s} the volume (L).

2.3 Simulations

The potential distribution, current flow, and induced charges were simulated by using COMSOL Multiphysics software package (COMSOL, Inc, Burlington, MA). The EC model reactor (1:1) was built in the electrostatic module of COMSOL. To visualize the electrostatic equilibrium phenomenon, the potential at the BPEs was fixed at 0 V (Pébère and Vivier, 2016) while the potential of driving anode and driving cathode electrode was set at $+10$ V and -10 V vs SHE, respectively. Then, the potential distribution, current flow, and electric charges were computed numerically by finite element method via the post-processing module of the COMSOL.

3 Results and discussion

3.1 Effect of BPE combination on EC performance

Figure 2 shows the electrochemical dissolution of Fe and Al with different combination of sacrificial electrodes during EC process. As shown in Fig. 2(a), Fe concentration reached 150.3 mg/L with Fe as driving anode (Fe-EC) after 10 min operation. With one Fe- or Al-BPE added into Fe-EC, Fe concentration increased by 29.4% or 18.9% than Fe-EC. While with two Fe-BPEs (Fe-WEC-2Fe/BPE), Fe concentration increased by 48.3% compared with Fe-EC, but less than twice of that with one Fe-BPE in (Fe-WEC-1Fe/BPE). With two Al-BPEs in Fe-EC (Fe-WEC-2Al/BPE) system, Fe concentration decreased by 12.7% compared with that of Fe-EC. Based on electric circuit principles, one BPE (Fe or Al) could be equivalent to a parallel branch in the Fe-EC circuit, which contributed to the increase of current flow in solution and electrochemical dissolution rate on Fe driving anode (Mavré et al., 2010). However, increasing the number of BPE could also result in a significant voltage drop on BPEs, and thus reduced electrochemical dissolution rate on the Fe driving anode.

Notably, with one Fe BPE and one Al BPE in Fe-EC system (Fe-WEC-1Fe/1Al/BPE) shown in Fig. 2(a), Fe concentration increased by 20.6% over that of Fe-WEC-1Fe/BPE while Al concentration decreased by 47.4% than that of Fe-WEC-1Al/BPE. A similar trend was also observed with Al driving electrode as illustrated in Fig. 2(b). In such case, mutual interference might occur among BPEs, which may be the most likely reason why the electrochemical dissolution of sacrificial electrodes (Fe or Al) was not increased proportionally with the increase in the number of BPEs. This assumption will also be demonstrated in Section 3.5.

3.2 Effect of BPE combination on pollutant removal

To investigate pollutant removal of each reactor with different BPEs configuration, the turbidity, total organic carbon (TOC), total phosphorus (TP), and total nitrogen (TN) were examined during electrolysis. As shown in Figs. 3(a)–3(d), for the reactor with BPEs, the removal

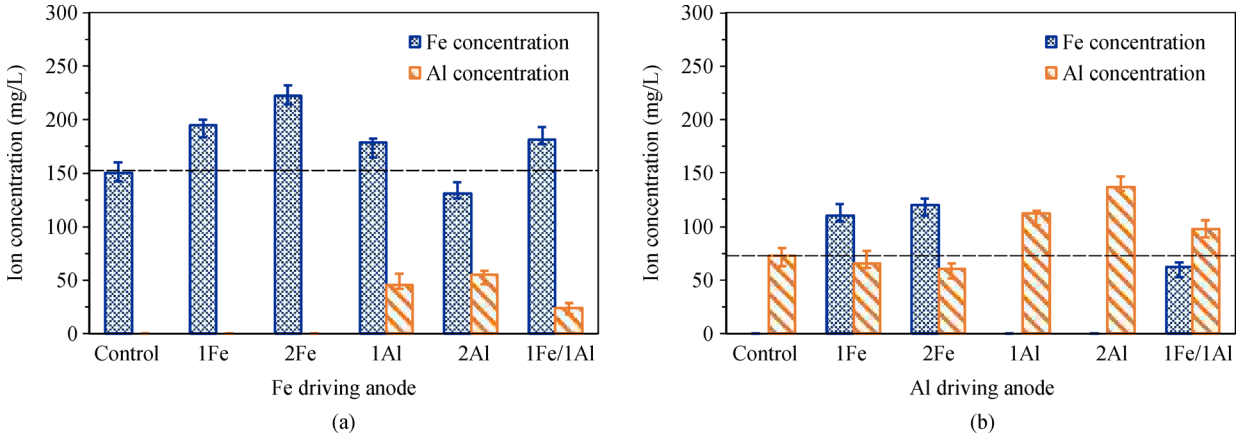

Fig. 2 Electrochemical dissolution of Al and Fe electrodes with different combination of sacrificial electrodes. (Control, 1Fe, 2Fe, 1Al, 2Al, 1Fe/1Al represent the operation systems of EC, WEC-1Fe/BPE, WEC-2Fe/BPE, WEC-1Al/BPE, WEC-2Al/BPE, WEC-1Fe/1Al/BPE, respectively at the applied current of 0.5 A and reaction time of 10 min).

efficiencies of turbidity, TOC, and TP were significantly higher than that of conventional EC (Figs. 3(a)–3(c)). Notably, TP removal reached 96.4% and 92.8% in Fe-WEC-2Al/BPE and Fe-WEC-2Fe/BPE respectively, the values being approximately 50% higher than that in conventional EC (Fig. 3(c)). A similar trend was also found for the case of Al serving as driving electrode (Figs. 3(a)–3(c)). This indicated that the addition of BPEs could improve EC performance, and thus remarkably enhance the removal of turbidity, TOC, and TP. The lowest final values of turbidity, TOC and TP were 7.4 NTU, 10.9 mg/L and 0.8 mg/L for Fe-WEC-2Al/BPE, Al-WEC-2Fe/BPE and Al-WEC-2Fe/BPE, respectively, which could meet the discharge standard of Class 1A, Class 1A and Class 1B, according to Chinese discharge standard of pollutants for municipal WWTPs (GB18918-2002) (Sun et al., 2016).

Noteworthy is that the increase of Fe and Al flocculated ions into the solution had a negligible impact to TN

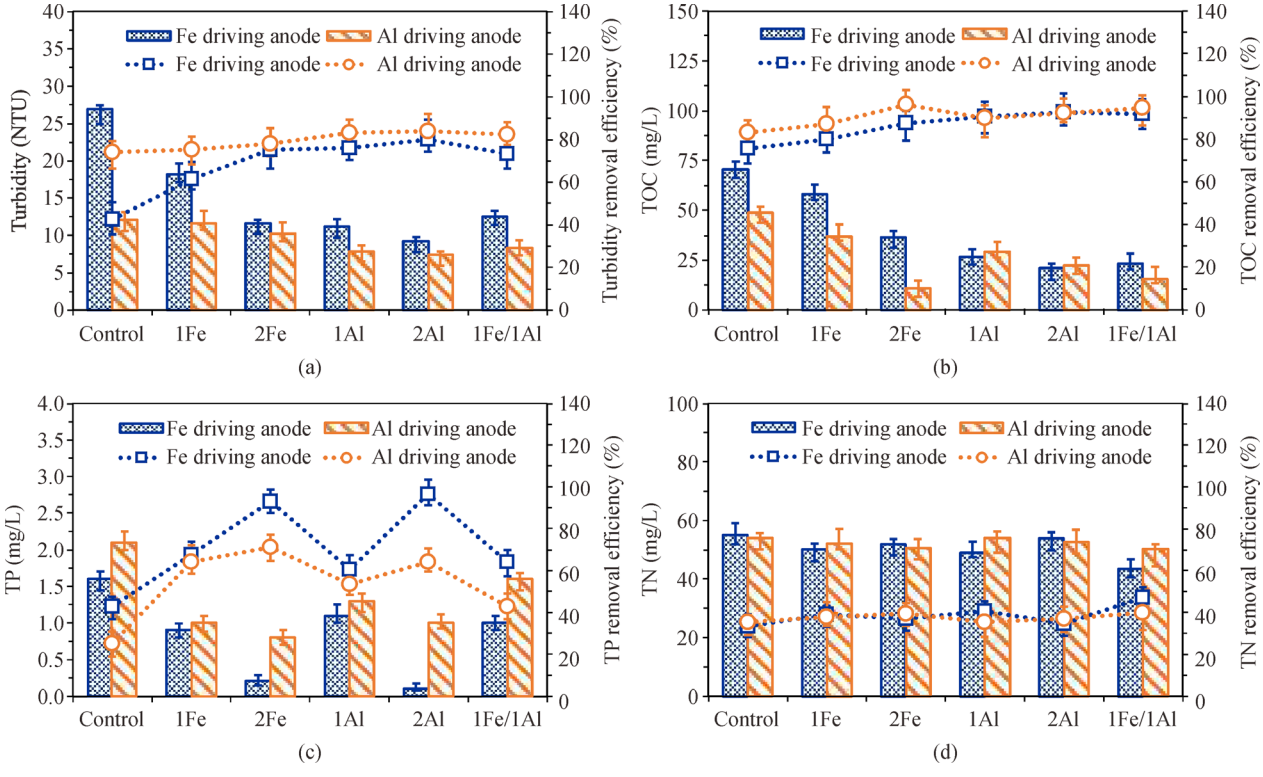

Fig. 3 Effect of integrations of EC and BPEs on the removal of (a) turbidity, (b) TOC, (c) TP and (d) TN of the municipal wastewater in 10 min.

removal and the maximum removal efficiency of TN was only 47.2% in Fe-WEC-1Fe/1Al/BPE (Fig. 3(d)). The most likely reason for this may be that the nitrogen species existing in different oxidation states (Reddy and Lin, 2000; Peel et al., 2003) are highly stable, making it more difficult be removed from wastewater. This indicated a limiting capability of electrocoagulation process for removal of nitrogen.

3.3 Voltage output with the addition of BPEs

Figure 4 shows the voltage output (V_{output}) of the cell during the electrocoagulation process with different configuration of BPEs. One can see that the voltage output did not change greatly with and without BPEs addition. The electrolytic cell with the same number of BPEs showed almost the same decrease in V_{output} compared with BPEs-free EC, which was independent on BPE material (Fig. 4). For example, for Fe serving as driving anode (Fig. 4(a)), the V_{output} was 16.4 V for EC, while the V_{output} value of 8.8 V was attained for Fe-WEC-2Al/BPE (i.e. 46.4% decrease). Likewise, for Al driving anode, 47.8% decline of V_{output} was obtained with the addition of two Fe- or Al- BPEs (Fig. 4(b)). This should be attributed to the changes of electric field and current flow in solution induced by the addition of BPEs as discussed below.

3.4 Energy consumption with the addition of BPEs

During removal of TOC and TP in electrocoagulation process (Fig. 3), the specific electric energy consumption (EEC) was investigated. As shown in Fig. 5, for either Fe or Al driving anode, the EEC value for TOC removal was approximately 5.8×10^{-3} kWh/(kgTOC), a value that accounted for 53.9% decrease compared with conventional EC (Fig. 5(a)). The EEC for TP removal in EC was 2.3×10^{-3} kWh/(kgTP) (Fig. 5(b)), the value being significantly lower than that for TOC (12.7×10^{-3} kWh/(kgTOC)) (Fig. 5(a)). The phosphorus ions were more soluble, and more easily to react with metal ions (Fe^{3+} and Al^{3+}) to form insoluble precipitates ($FePO_4$ or $AlPO_4$) (Eq. (2) and (3)) (Mahvi et al., 2011).

$$Al^{3+} + PO_4^{3-} \rightarrow AlPO_4 \downarrow \quad (2)$$

$$Fe^{3+} + PO_4^{3-} \rightarrow FePO_4 \downarrow \quad (3)$$

Moreover, for two Fe-BPEs, the EEC for TP removal was decreased by 75.3% in Fe-WEC-2Fe/BPE and 81.5% in Al-WEC-2Fe/BPE than that in EC (Fig. 5(b)). This is most likely due to the addition of BPEs driven by electric field to release Fe or Al ions into solution and form more flocs with negligible pH change of solution (Fig. S2), which may have a contribution to improved TOC/TP removal and declined EEC. Besides, the EDS spectra of precipitates produced in Fe-WEC-2Fe and Fe-WEC-2Al illustrate the main composition of Fe and Al involved in the precipitates (Fig. S3), suggesting the possibility to recycle metals (Fe and Al) from precipitates to prevent secondary pollution. Therefore, EC integrated with BPEs may be used as a potential choice to achieve enhanced wastewater treatment and at the same time lower energy consumption without additional wire connection and complicated modification.

3.5 Simulation of electric field

To better understand the distribution of potential and current density on BPEs in accordance with the results shown in Fig. 2 and Fig. 3, we performed the numerical simulations using COMSOL software based on finite element method. The driving voltage of 20 V was

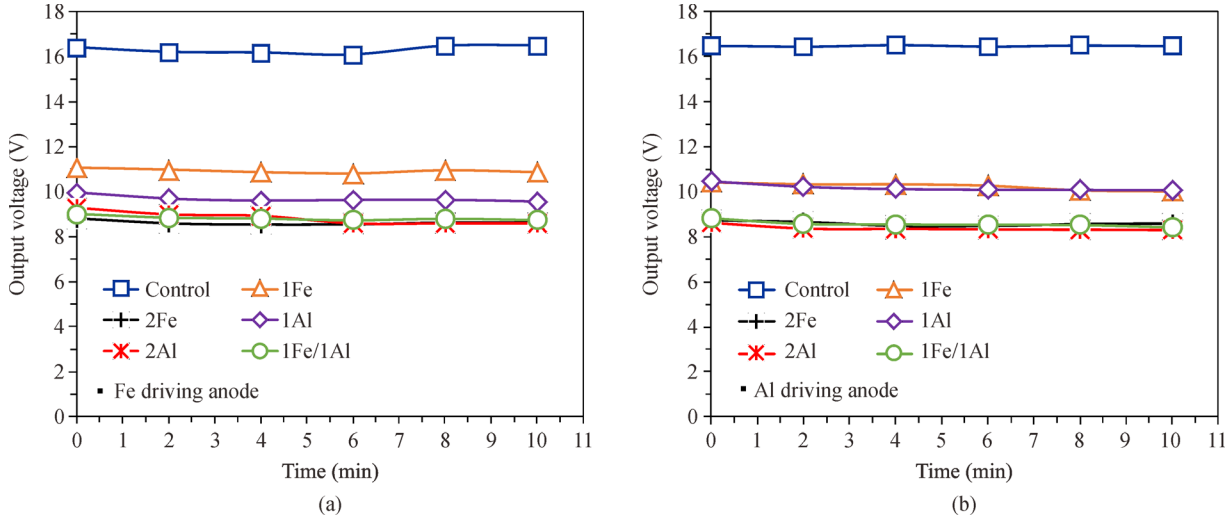

Fig. 4 Cell voltage during the electrocoagulation for (a) Fe driving anode and (b) Al driving anode with different BPEs combinations under constant current of 0.5 A.

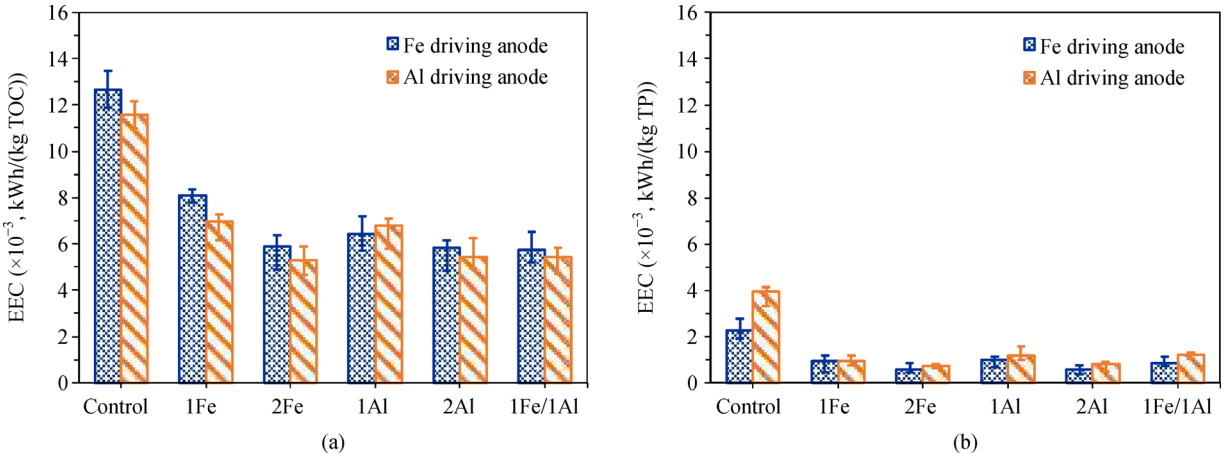

Fig. 5 Electric energy consumption for removal of (a) TOC and (b) TP with different configuration of BPEs.

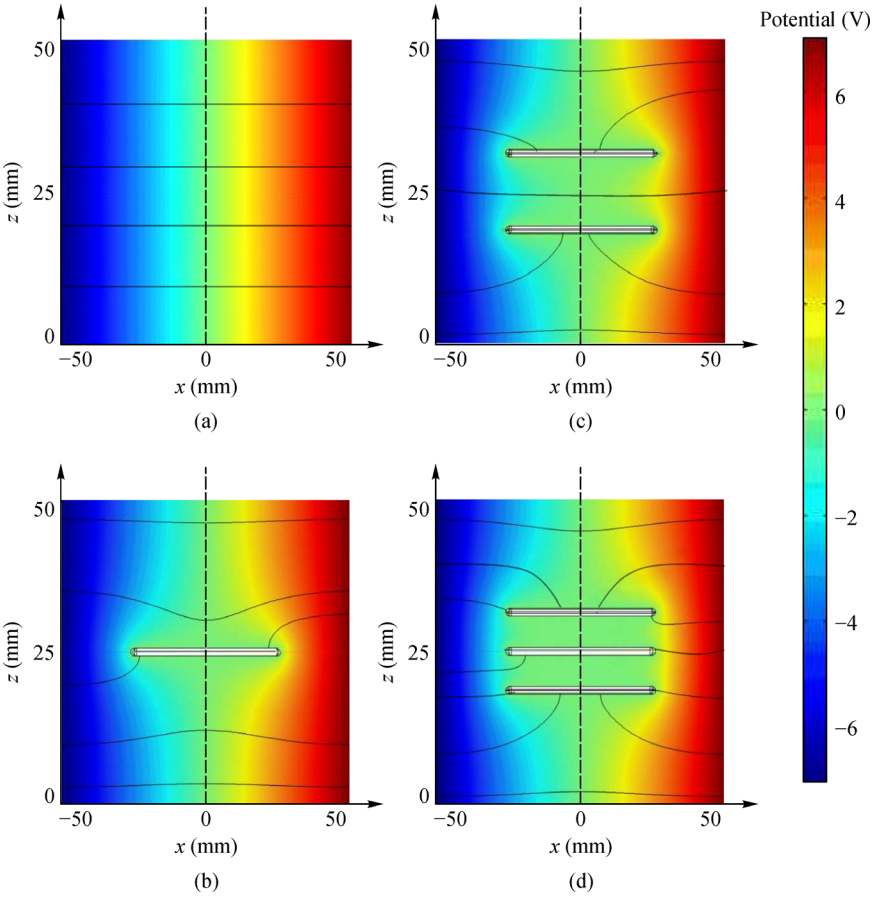

Fig. 6 Simulation of distribution of potential and current flow in the solution of EC system integrated with (a) zero, (b) one, (c) two and (d) three BPEs in the x–z plane.

employed to mitigate the impact of insufficient voltage to simulation results (Pébère and Vivier, 2016). In the presence of an electric field, the electrostatic balance of a conductor is independent on the material (Li et al., 2018), and hence the driving electrodes and BPEs were all set with iron conductor. The simulation was carried out based on the assumption that the redox reactions on the surface of electrodes had negligible impact to initial excited state.

Figure 6 shows the simulation results based on zero, one, two, and three BPEs in the $x-z$ plane. In the absence of BPEs, the simulated current flow (black lines) was seen even and parallel (Fig. 6(a)), indicating a constant current

density and electric field in the solution of EC system. According to Ohm's law, the actual distribution of current can be estimated from the potential gradient being perpendicular to the driving electrodes (Ryder, 1953). However, the center of symmetry locates on zero potential surface of the BPE (x = 0, Figs. 6(b)–6(d)). The current flow in solution became uneven and some flowed directly through BPE, indicating that the redox reactions were taking place on the surface of BPE in this region. In such case, higher electric currents produced on two BPEs driven by electric field were equivalent to that caused by an additional ionic current in the solution, which lowered ohmic resistance and charge transfer resistance in the solution. Thus, the decrease in voltage output and energy consumption was in line with the results shown in Fig. 4 and Fig. 5.

In Fig. 6(c), two BPEs led to partial changes of the potential and current distribution in solution and the same current flowing through them. Notably, three BPEs not only caused the changes of potential and current distribution in solution, but also induced significantly mutual effect between BPEs (Fig. 6(d)). An uneven distribution of current flow was induced on three BPEs, and the current flowing through the middle BPE was less than that of the other two ones (Fig. 6(d)).

As shown in Fig. 7, the red arrows indicated the induced charges whose length and density depended on the charge intensity induced on BPE surface, and the direction was as same as the electric field of the solution. As shown in Fig. 7(b), at the positon of x = 0, the potential was zero, indicating no induced charge. The profile of x = 0 divided the BPE to two poles, i.e. the anodic pole ($x < 0$) and cathodic pole ($x > 0$). The maximum length and density of charges were located at two edges of each BPE, which descended linearly toward the middle of BPE (x = 0). According to Faraday's Law (Barker and Walsh, 1991; Walsh, 1991),

$$m = \frac{q_{\mathrm{M}}}{nF}, \tag{4}$$

where q_{M} is the charge passed the circuit, n the number of charge involved in electrochemical reaction, F the Faraday's constant (96485 C/mol), and m the amount of material reacted. Thus, the corresponding distribution of redox reaction rates on BPE surface could be expressed by Eq. (4). The maximum of redox reaction rate was found at both ends of each BPE, which decreased gradually toward the middle position of BPE (x = 0). In addition, the evolution of corrosion morphology along the length of one BPE confirmed the occurrence of redox reaction (Fig. 8).

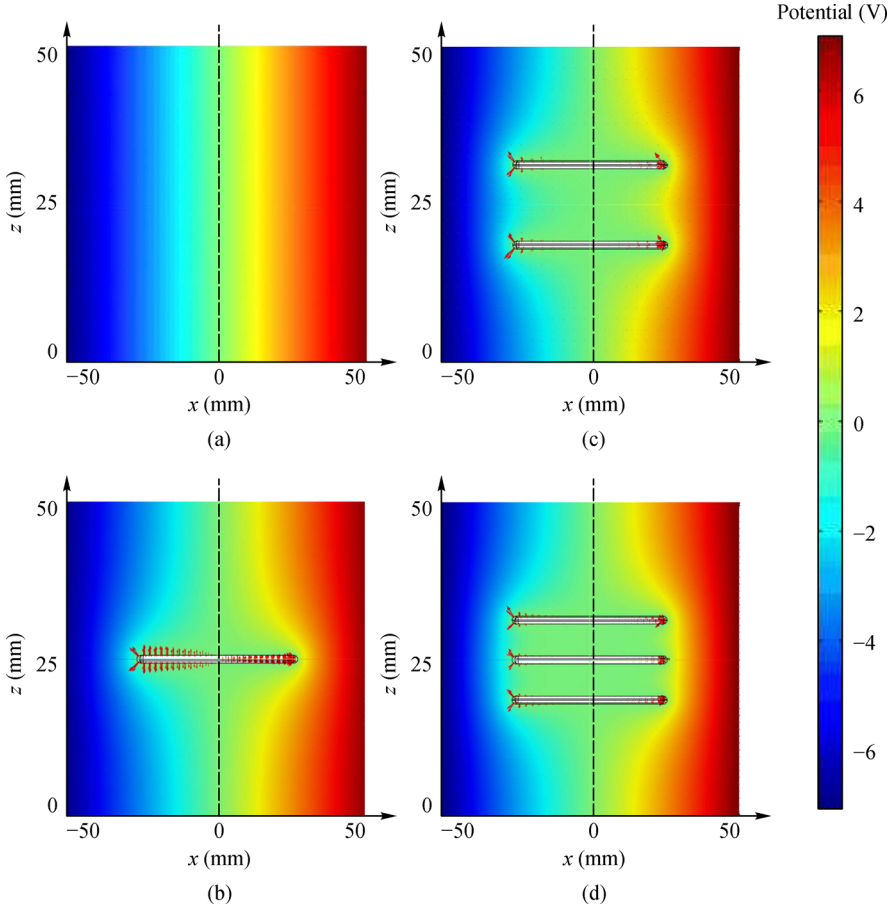

Fig. 7 Simulation of distribution of charges on the surface of (a) zero, (b) one, (c) two and (d) three BPEs in the x–z plane.

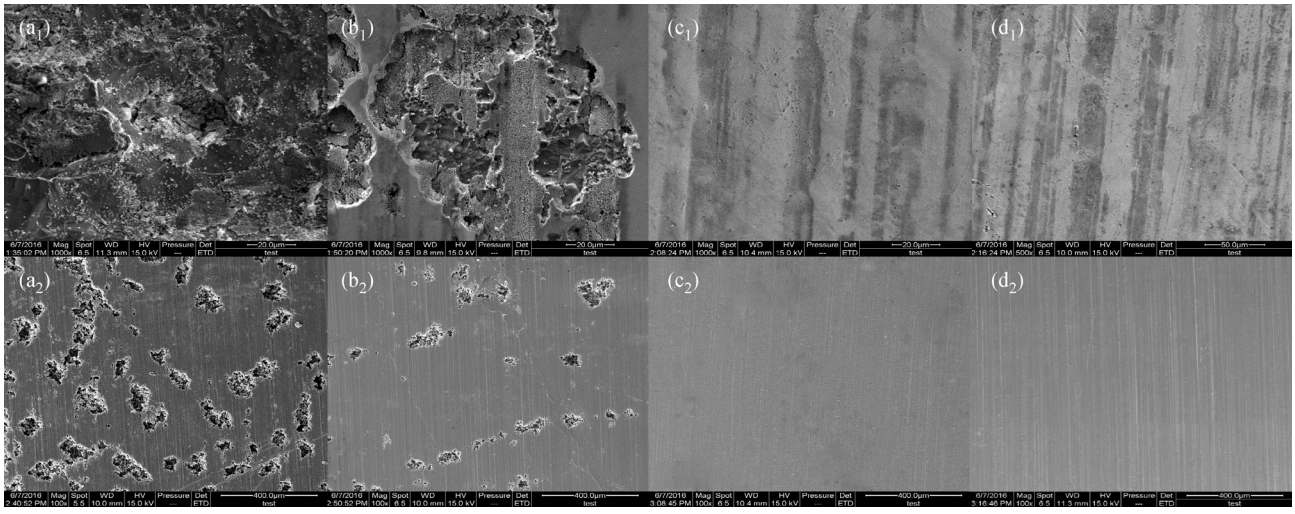

Fig. 8 SEM images of corrosion morphology along the length of horizontal Fe/BPE at location of (a_1) 0 mm, (b_1) 10 mm, (c_1) 40 mm and (d_1) 50 mm; along the length of horizontal Al/BPE at the location of (a_2) 0 mm, (b_2) 10 mm, (c_2) 40 mm and (d_2) 50 mm distanced from the anodic end. (Fe-WEC-1Fe/1Al/BPE system, reaction time of 10 min).

As shown in Figs. 6(b) – 6(d), the density of the charges induced on two or three BPEs was obviously lower than that on single BPE. This was because of the correlation between the charge transfer rate on electrode/solution interface and redox rate (Jüttner et al., 2000; Mansouri et al., 2011; Cho et al., 2014). This might provide the most probable explanation to the fact that increasing the number of BPEs increased the reaction rate to a certain extent but could not multiply that of one BPE as reported in our previous studies (Qi et al., 2017, 2018).

The simulation result of charge distribution on three BPEs presents an overview of the dual impact of two BPEs on the middle one (Fig. 7(d)). The one in the middle of the three BPEs was shown to be strongly affected by addition of other two BPEs, indicated by visible inductive charges at its edges. As a result, the redox reaction rate on the middle BPE became much lower than that of the other two BPEs. Based on the electrostatic theory, the interaction between BPEs should result from the electrostatic field on surface of BPEs, which was responsible for the decreased redox reaction rate on each BPE with increasing the number of BPEs. To further verify this anticipation, the theoretical simulation of surface charge distribution was studied in the $x-y$ plane.

As shown in Fig. 9(a), in electrostatic equilibrium state, the induced charge on BPE surface was perpendicular to the surface, and the positive charge was concentrated in the anodic pole while the negative charge in cathodic pole. In electrostatic balance state, the BPEs were equipotential bodies with equipotential surface (Keddam et al., 2009). Thus, there was no charge accumulated inside the BPE conductor, and the induced charge remained on BPE surface being perpendicular to the direction of the external field intensity (Fig. 9(a)).

According to Gauss theorem, the surface electric field intensity was proportional to the surface charge density as (Bonnor, 1953; Szabó et al., 2006):

$$E = \frac{\sigma}{\varepsilon_0}, \tag{5}$$

where ε_0 is the electrolyte constant of a vacuum, the surface density of charge at a point in the conductor surface, and E the electric field intensity at specific point. As shown in Eq. (5), the induced electric field intensity on BPE surface decreased from the two ends of BPE ($x = \pm 25$) to the geometrical center ($x = 0$), which affected both the external electric field near its surface and the induced electric field on the adjacent BPEs (Fig. 9(a)). As illustrated in Fig. 9(b), the electric field force drives the charges to directionally induce redox reactions via consuming electric field energy and generating an extra current (i_{bpe}) on the BPE surface (Marcus, 1956; Chang et al., 2012). Therefore, combining BPE with EC may offer an alternative way to enhance electrochemical dissolution rate for producing more flocculation ions and lowering electric energy input during municipal wastewater treatment. Since redox reaction rate strongly depends on distribution of induced charges on BPE surface during EC process, simulation methodology may also be a useful tool for optimizing reactor design, predicting EC performance and improving energy efficiency.

4 Conclusions

In this study, an EC system was augmented with BPEs to enhance pollutant removal and reduce energy consumption for real municipal wastewater treatment. Based on above results, main conclusions can be drawn as follows.

1) In EC with two Al-BPEs, the removal efficiency

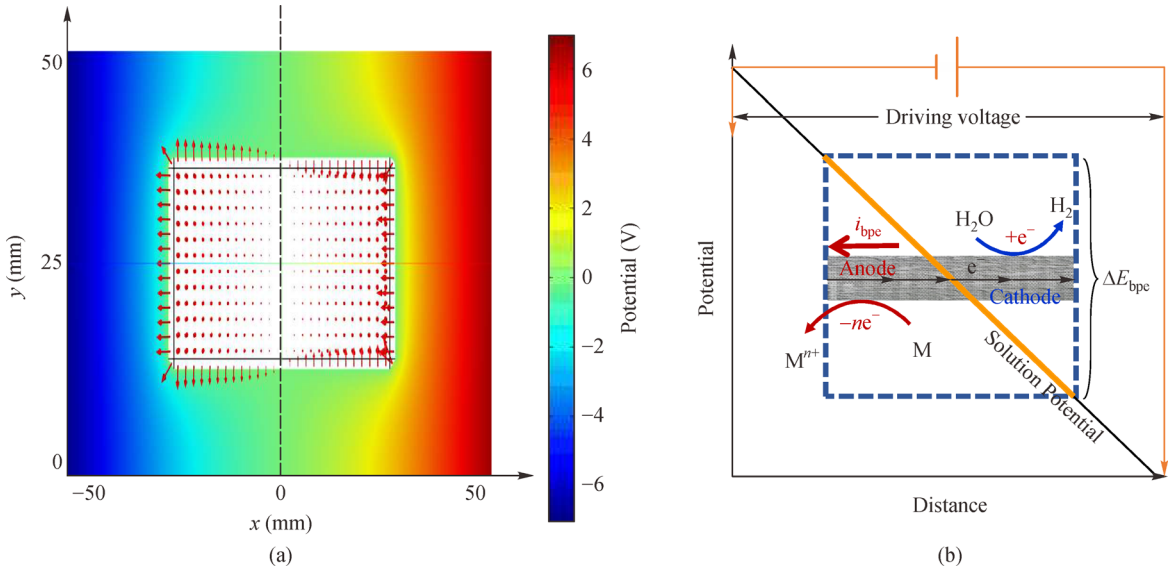

Fig. 9 (a) Simulation of induced charges on Fe-BPE surface in the *x*–*y* plane, (b) Schematic diagram of side-view mechanism in the *x*–*z* plane.

increased by 60.4% and 17.1% for turbidity and TOC, respectively, compared with BPE-free EC. Moreover, the removal efficiency of TP could reach 96.4%, a value 50% higher than that obtained with conventional EC in 10-min operations.

2) With two BPEs (especially two Fe-BPEs) in EC, the energy consumption for TP removal decreased by 75.2% with Fe driving anode and 81.5% with Al driving anode than BPE-free EC.

3) The yield of flocculation ions significantly increased with increased number of BPEs, but not proportionally due to the mutual interaction between BPEs.

4) The simulation results provided a visual illustration of the distribution of potential and current in solution, the induced charges on BPEs surface and the mutual effect among BPEs.

Acknowledgements Project supported by the National Natural Science Foundation of China (Grant Nos. 51822806, 51678184 and 51761145031), and Fundamental Research Funds for the Central Universities (Grant HIT. BRETIV.201905).

Electronic Supplementary Material Supplementary material is available in the online version of this article at https://doi.org/10.1007/s11783-020-1215-3 and is accessible for authorized users.

References

Al-Shannag M, Bani-Melhem K, Al-Anber Z, Al-Qodah Z (2013). Enhancement of COD-nutrients removals and filterability of secondary clarifier municipal wastewater influent using electrocoagulation technique. Separation Science and Technology, 48(4): 673–680

Bani-Melhem K, Al-Shannag M, Alrousan D, Al-Kofahi S, Alqodah Z, Al-Kilani M R (2017). Impact of soluble COD on grey water treatment by electrocoagulation technique. Desalination and Water Treatment, 89: 101–110

Barker D, Walsh F C (1991). Applications of Faraday's laws of electrolysis in metal finishing. Transactions of the IMF, 69(4): 158–162

Bhatti M S, Reddy A S, Kalia R K, Thukral A K (2011). Modeling and optimization of voltage and treatment time for electrocoagulation removal of hexavalent chromium. Desalination, 269(1–3): 157–162

Bhatti M S, Reddy A S, Thukral A K (2009). Electrocoagulation removal of Cr(VI) from simulated wastewater using response surface methodology. Journal of Hazardous Materials, 172(2–3): 839–846

Bonnor W B (1953). Certain exact solutions of the equations of general relativity with an electrostatic field. Proceedings of the Physical Society. Section A, 66(2): 145

Chang B Y, Chow K F, Crooks J A, Mavré F, Crooks R M (2012). Two-channel microelectrochemical bipolar electrode sensor array. Analyst (London), 137(12): 2827–2833

Chavalparit O, Ongwandee M (2009). Optimizing electrocoagulation process for the treatment of biodiesel wastewater using response surface methodology. Journal of Environmental Sciences (China), 21 (11): 1491–1496

Cho K, Kwon D, Hoffmann M R (2014). Electrochemical treatment of human waste coupled with molecular hydrogen production. RSC Advances, 4(9): 4596–4608

Chow K F, Mavré F, Crooks J A, Chang B Y, Crooks R M (2009). A large-scale, wireless electrochemical bipolar electrode microarray. Journal of the American Chemical Society, 131(24): 8364–8365

Daneshvar N, Ashassi Sorkhabi H, Kasiri M B (2004). Decolorization of dye solution containing Acid Red 14 by electrocoagulation with a comparative investigation of different electrode connections. Journal of Hazardous Materials, 112(1–2): 55–62

Gao S, Yang J, Tian J, Ma F, Tu G, Du M (2010). Electro-coagulation–flotation process for algae removal. Journal of Hazardous Materials, 177(1–3): 336–343

Garcia-Segura S, Eiband M M S, de Melo J V, Martínez-Huitle C A

(2017). Electrocoagulation and advanced electrocoagulation processes: A general review about the fundamentals, emerging applications and its association with other technologies. Journal of Electroanalytical Chemistry, 801: 267–299

Ghosh D, Medhi C R, Purkait M K (2008). Treatment of fluoride containing drinking water by electrocoagulation using monopolar and bipolar electrode connections. Chemosphere, 73(9): 1393–1400

Hakizimana J N, Gourich B, Chafi M, Stiriba Y, Vial C, Drogui P, Naja J (2017). Electrocoagulation process in water treatment: A review of electrocoagulation modeling approaches. Desalination, 404: 1–21

Jiang J Q, Graham N, André C, Kelsall G H, Brandon N (2002). Laboratory study of electro-coagulation–flotation for water treatment. Water Research, 36(16): 4064–4078

Jiménez C, Sáez C, Cañizares P, Rodrigo M A (2016). Optimization of a combined electrocoagulation-electroflotation reactor. Environmental Science and Pollution Research International, 23(10): 9700–9711

Jüttner K, Galla U, Schmieder H (2000). Electrochemical approaches to environmental problems in the process industry. Electrochimica Acta, 45(15–16): 2575–2594

Keddam M, Nóvoa X R, Vivier V (2009). The concept of floating electrode for contact-less electrochemical measurements: Application to reinforcing steel-bar corrosion in concrete. Corrosion Science, 51 (8): 1795–1801

Kobya M, Bayramoglu M, Eyvaz M (2007). Techno-economical evaluation of electrocoagulation for the textile wastewater using different electrode connections. Journal of Hazardous Materials, 148 (1–2): 311–318

Li M, Liu S, Jiang Y, Wang W (2018). Visualizing the zero-potential line of bipolar electrodes with arbitrary geometry. Analytical Chemistry, 90(11): 6390–6396

Mahvi A H, Ebrahimi S J A D, Mesdaghinia A, Gharibi H, Sowlat M H (2011). Performance evaluation of a continuous bipolar electrocoagulation/electrooxidation–electroflotation (ECEO–EF) reactor designed for simultaneous removal of ammonia and phosphate from wastewater effluent. Journal of Hazardous Materials, 192(3): 1267–1274

Mansouri K, Ibrik K, Bensalah N, Abdel-Wahab A (2011). Anodic dissolution of pure Aluminum during electrocoagulation process: Influence of supporting electrolyte, initial pH, and current density. Industrial & Engineering Chemistry Research, 50(23): 13362–13372

Marcus R A (1956). On the theory of oxidation-reduction reactions involving electron transfer. I. Journal of Chemical Physics, 24(5): 966–978

Martinez-Delgadillo S, Mollinedo-Ponce H, Mendoza-Escamilla V, Gutiérrez-Torres C, Jiménez-Bernal J, Barrera-Diaz C (2012). Performance evaluation of an electrochemical reactor used to reduce Cr(VI) from aqueous media applying CFD simulations. Journal of Cleaner Production, 34: 120–124

Mavré F, Anand R K, Laws D R, Chow K F, Chang B Y, Crooks J A, Crooks R M (2010). Bipolar electrodes: A useful tool for concentration, separation, and detection of analytes in microelectrochemical systems. Analyst (London), 82: 8766–8774

Modirshahla N, Behnajady M A, Mohammadi-Aghdam S (2008). Investigation of the effect of different electrodes and their connections on the removal efficiency of 4-nitrophenol from aqueous solution by electrocoagulation. Journal of Hazardous Materials, 154 (1–3): 778–786

Mollah M Y A, Schennach R, Parga J R, Cocke D L (2001). Electrocoagulation (EC)—Science and applications. Journal of Hazardous Materials, 84(1): 29–41

Mollah M Y, Morkovsky P, Gomes J A, Kesmez M, Parga J, Cocke D L (2004). Fundamentals, present and future perspectives of electrocoagulation. Journal of Hazardous Materials, 114(1–3): 199–210

Moussa D T, El-Naas M H, Nasser M, Al-Marri M J (2017). A comprehensive review of electrocoagulation for water treatment: Potentials and challenges. Journal of Environmental Management, 186: 24–41

Olmez-Hanci T, Kartal Z, Arslan-Alaton İ (2012). Electrocoagulation of commercial naphthalene sulfonates: process optimization and assessment of implementation potential. Journal of Environmental Management, 99: 44–51

Pébère N, Vivier V (2016). Local electrochemical measurements in bipolar experiments for corrosion studies. ChemElectroChem, 3(3): 415–421

Peel J W, Reddy K J, Sullivan B P, Bowen J M (2003). Electrocatalytic reduction of nitrate in water. Water Research, 37(10): 2512–2519

Qi Z, You S, Ren N (2017). Wireless electrocoagulation in water treatment based on bipolar electrochemistry. Electrochimica Acta, 229: 96–101

Qi Z, Zhang J, You S (2018). Effect of placement angles on wireless electrocoagulation for bipolar aluminum electrodes. Frontiers of Environmental Science & Engineering, 12(3): 9

Reddy K J, Lin J (2000). Nitrate removal from groundwater using catalytic reduction. Water Research, 34(3): 995–1001

Ryder E J(1953). Mobility of holes and electrons in high electric fields. Physical Review, 90(5): 766

Sahu O, Mazumdar B, Chaudhari P K (2014). Treatment of wastewater by electrocoagulation: A review. Environmental Science and Pollution Research International, 21(4): 2397–2413

Sun Y, Chen Z, Wu G, Wu Q, Zhang F, Niu Z, Hu H Y (2016). Characteristics of water quality of municipal wastewater treatment plants in China: Implications for resources utilization and management. Journal of Cleaner Production, 131: 1–9

Szabó T, Tombácz E, Illés E, Dékány I (2006). Enhanced acidity and pH-dependent surface charge characterization of successively oxidized graphite oxides. Carbon, 44(3): 537–545

Vázquez A, Nava J L, Cruz R, Lázaro I, Rodríguez I (2014). The importance of current distribution and cell hydrodynamic analysis for the design of electrocoagulation reactors. Journal of Chemical Technology and Biotechnology (Oxford, Oxfordshire), 89(2): 220–229

Vázquez A, Rodríguez I, Lázaro I (2012). Primary potential and current density distribution analysis: A first approach for designing electrocoagulation reactors. Chemical Engineering Journal, 179: 253–261

Walsh F C (1991). The overall rates of electrode reactions: Faraday's laws of electrolysis. Transactions of the IMF, 69(4): 155–157

Zhang X, Shang C, Gu W, Xia Y, Li J, Wang E (2016). A renewable display platform based on the bipolar electrochromic electrode. ChemElectroChem, 3(3): 383–386